

**TICRA**  
engineering consultants  
communications systems and antennas

RF effect  
of core print-through distortion  
on the Planck telescope

Marts, 2000

S-801-05

Author:

Per Heighwood Nielsen



## TABLE OF CONTENTS

|  |    |
|--|----|
| 1. INTRODUCTION .....                                    | 2  |
| 2. CORE PRINT-THROUGH MODEL .....                        | 3  |
| 3. RF EFFECTS OF CORE DEPTH-THROUGH SURFACE ERRORS ..... | 5  |
| 3.1 Distortions on primary mirror .....                  | 6  |
| 3.2 Distortions on secondary mirror .....                | 10 |
| 4. FREQUENCY DEPENDENCE .....                            | 14 |
| 5. REFERENCES .....                                      | 15 |

## 1. INTRODUCTION

The RF degradation of a periodic surface distortion structure as the core print-through is investigated in this report. The model of the core print-through distortion is presented in Chapter 2.

The RF performance of the distorted system is calculated with the GRASP8 program at the highest frequency 857 GHz for one of the centre horns, HFI857-1, and with two core print-through sizes. The horn is modelled as a simple Gaussian feed with the taper given in Table 4.6.a in the Alcatel Doc. No. PLAS TN 009.

The geometry of the aplanatic ALCATEL design, denoted CASE No. 1, is defined in ESA Doc. No. PT-DS-07024 and shown in Figure 1-1.

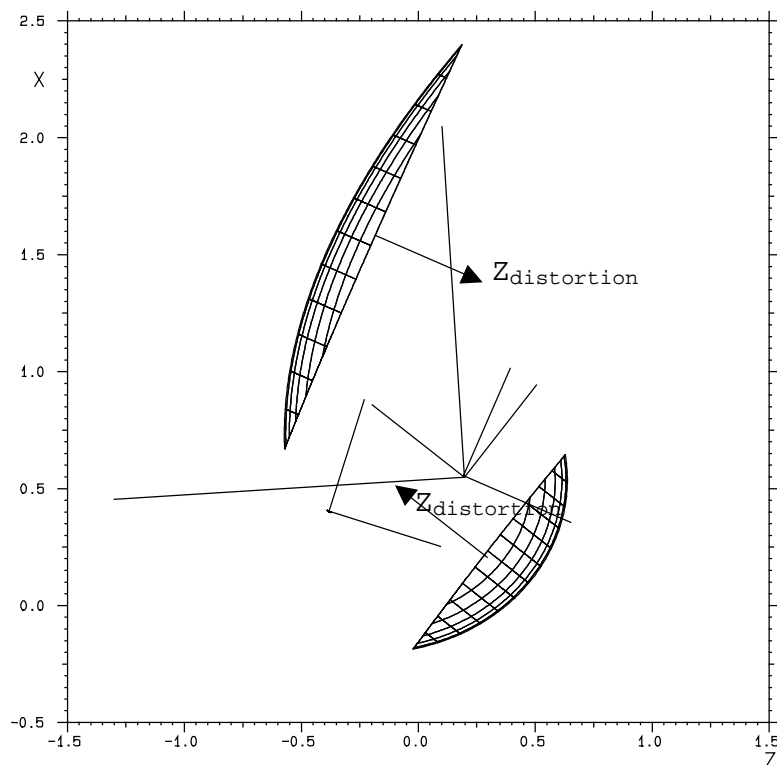


Figure 1-1 Geometry of aplanatic antenna system.

The RF degradations due to peaks of  $10\mu$  and  $2\mu$  of the core print-through distortions on both the primary and the secondary mirror are presented in Chapter 3.

## 2. CORE PRINT-THROUGH MODEL

The core print-through distortion is modelled as a second order function limited by a triangle with side length of 40 mm, see Figure 2-1.

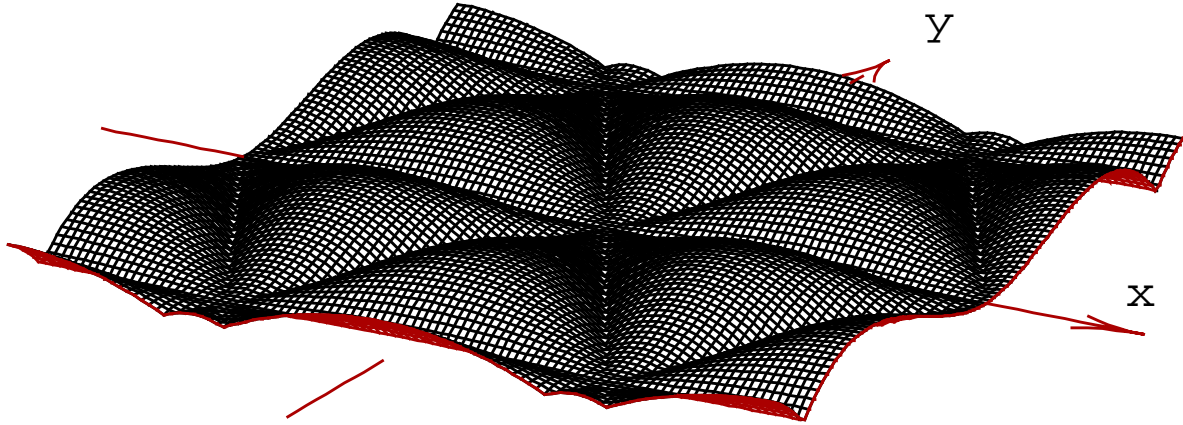


Figure 2-1 Core print-through surface distortion.

The surface function is defined in the space between the unit vectors  $\hat{s}$  and  $\hat{t}$  in Figure 2-2 by the following equation (2.1).

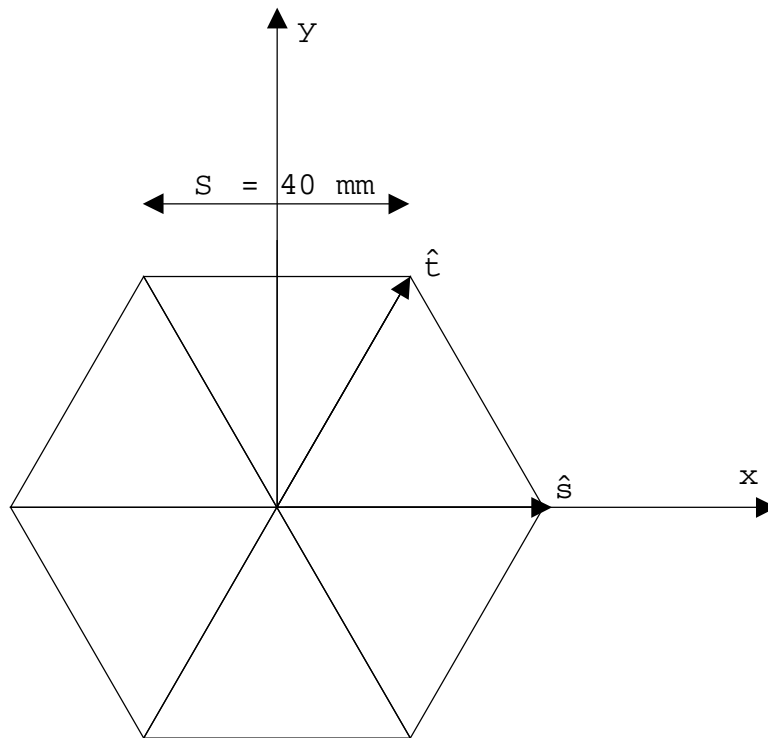


Figure 2-2 Core print-through co-ordinate system.

---

$$f(s, t) = 27. * \text{peak} * (st - (st^2 + s^2t)) \quad (2.1)$$

This equation fulfils the border conditions and the symmetry requirements, and the peak is positioned in  $s=t=1/3$ .

The distortion is added to the nominal surface of the mirrors in the direction of the normal to the rim planes, see Figure 1-1.

### 3. RF EFFECTS OF CORE DEPTH-THROUGH SURFACE ERRORS

The two-dimensional periodic structure of the core depth-through surface distortion gives rise to grating lobes in the far field. The  $\theta$  direction of the grating lobes,  $\theta_{gr}$ , can be found by

$$\sin \theta_{gr} = \frac{2\lambda}{S} \quad \text{for } \phi=0^\circ + p*60^\circ \quad (3.1)$$

and

$$\sin \theta_{gr} = \frac{2\lambda}{S\sqrt{3}} \quad \text{for } \phi=30^\circ + p*60^\circ \quad (3.2)$$

where  $\lambda$  is the wavelength and  $S$  is the side length.

The pattern is therefore calculated in the direction of the largest grating lobes, i.e. in the three cuts  $\phi=0^\circ$ ,  $30^\circ$  and  $90^\circ$ . The  $\theta, \phi$  direction is referenced to an output co-ordinate system in the direction of the main beam, and with the  $\phi=0^\circ$  plane in the antenna symmetry plane, see Figure 1-1 and Figure 2-2. If the core print-through distortion is rotated the grating lobes will be rotated by the same amount. The far field is also presented as contour curves in a UV grid, where the centre is in the main beam direction. The contour curves are drawn for several field levels 10 dB, 20 dB, 30 dB, ..., 90 dB below main peak.

The RF degradations are calculated for two different peaks of the core print-through distortion,  $10 \mu$  and  $2 \mu$ , and on the primary- and the secondary mirror as described in Section 3.1 and 3.2, respectively.

### 3.1 Distortions on primary mirror

The phase degradation of the primary mirror aperture field at 857 GHz and with 10 $\mu$  peak on core depth-through is shown in Figure 3-1.

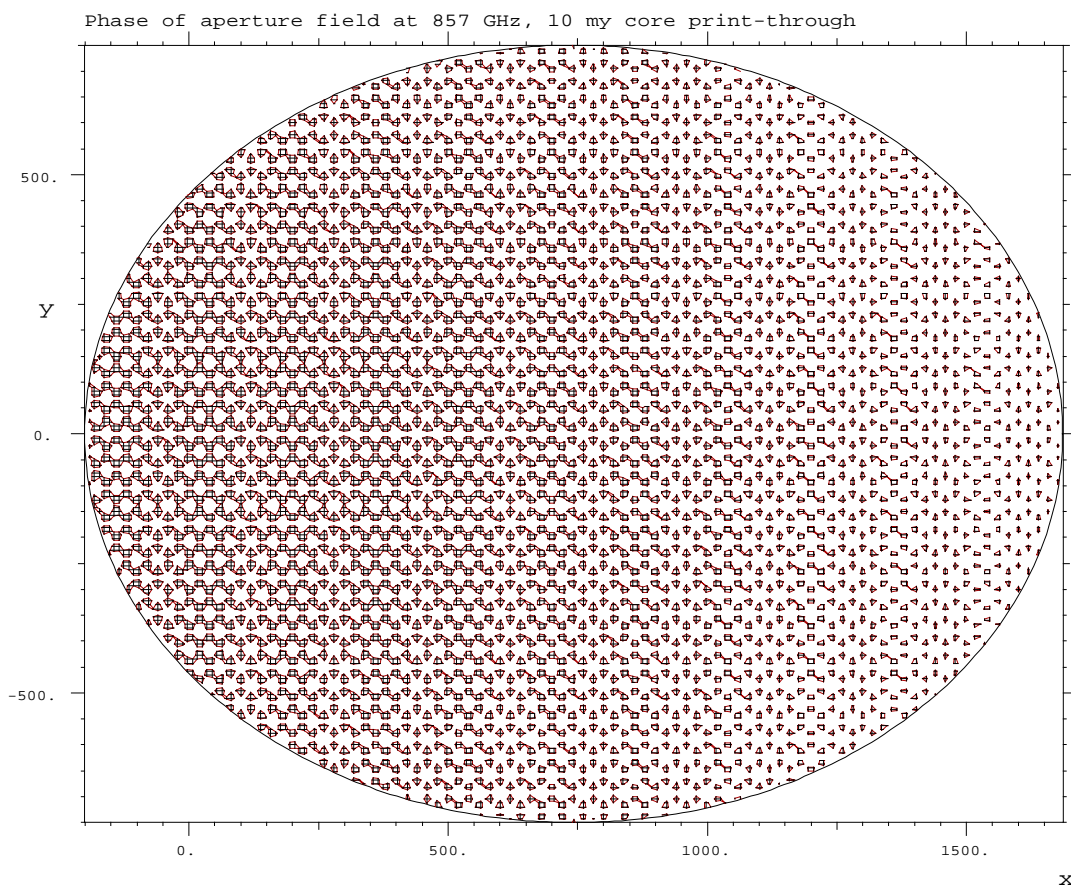
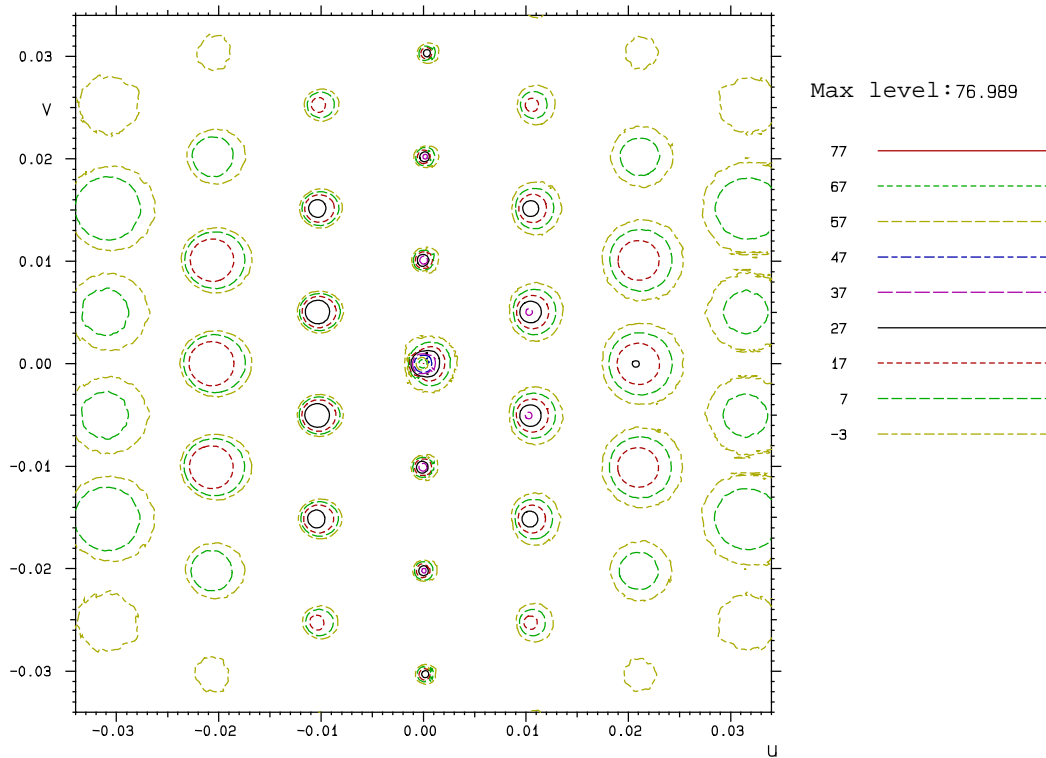


Figure 3-1 Aperture field phase error created by 10 $\mu$  peak on primary mirror.

The contour curves are drawn for a phase degradation of 10°. The maximum level is 18.8°. The phase peak variance in x is due to the offset geometry giving a different relation between the phase and the surface distortion over the aperture.

The far field from the periodic phase degradation is shown in a region of 2° around the main beam in Figure 3-2a. The main beam is only reduced by 0.03 dB, but large grating lobes are generated in a hexagonal grid around the main beam. The largest is in the  $\phi = 90^\circ$  plane at  $\theta = .58^\circ$  ( $v=.0101$ ) with a peak of

45.3 dBi, which is only 32 dB below the main beam peak. The most important grating lobes are also shown in the pattern cuts in Figure 3-2b. Due to the offset configuration the  $\phi$  directions are not exactly in the symmetry planes. The pattern is therefore calculated in the three cuts,  $\phi=0^\circ$ ,  $26^\circ$  and  $90^\circ$ . The  $\theta$  direction of the grating lobes agrees very well with the equations (3.1) and (3.2) keeping in mind that the projected S value is not 40 mm in the offset plane but reduced to 33 mm. When the core print through peak is reduced to  $2\mu$  the grating lobes are reduced by  $20\log(10\mu/2\mu)$  dB = 14 dB as shown in Figure 3-3.



a) uv pattern

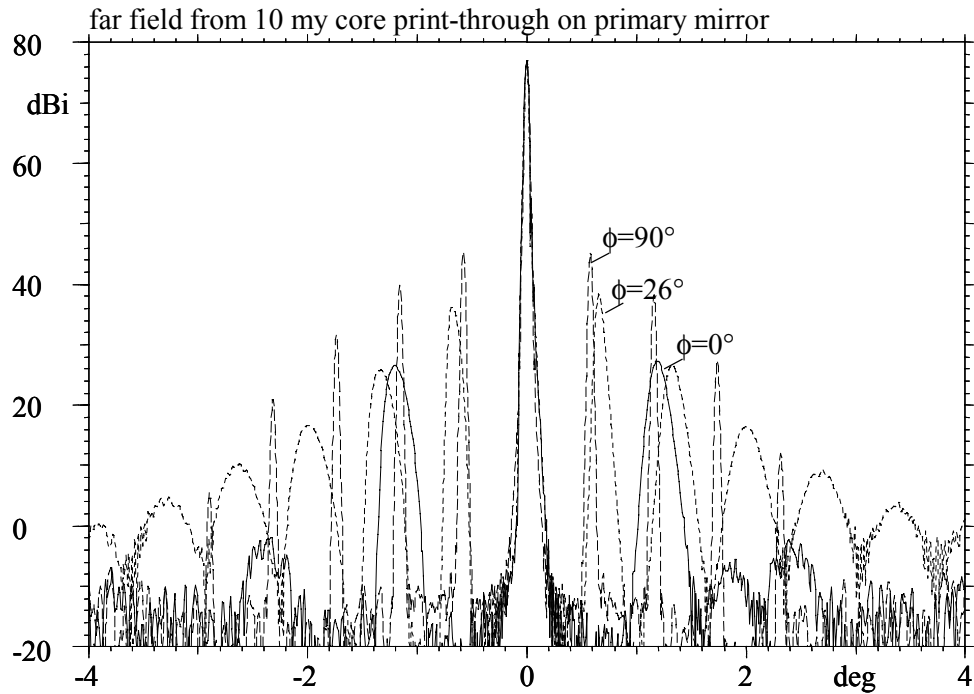
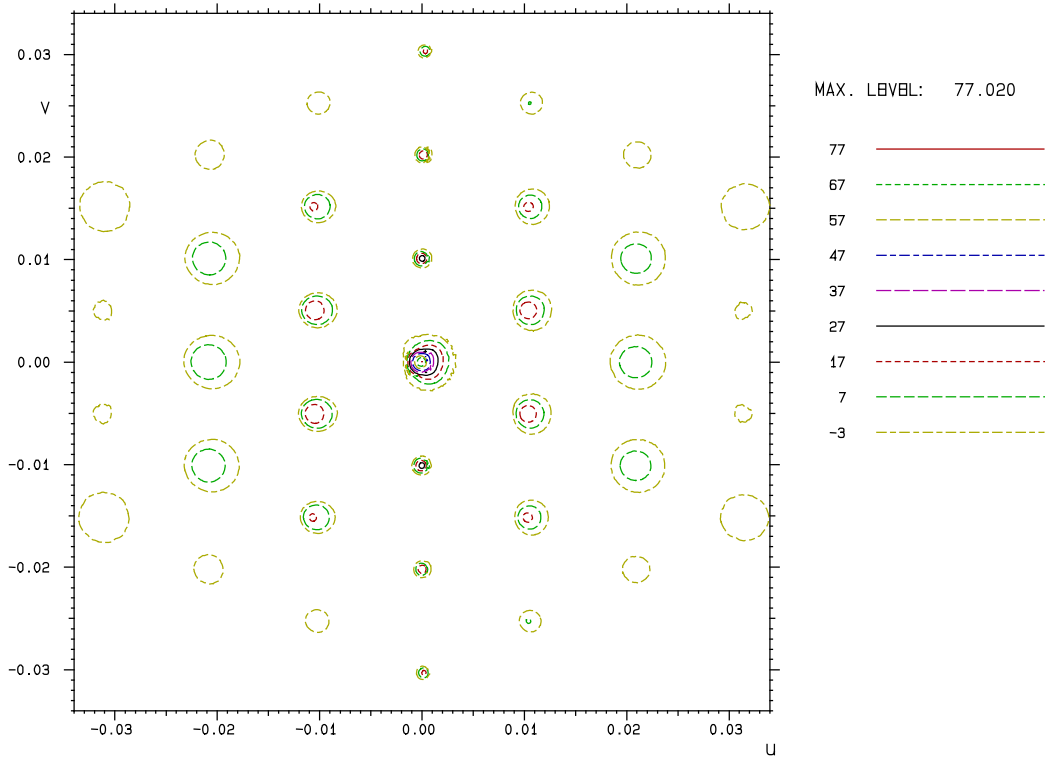
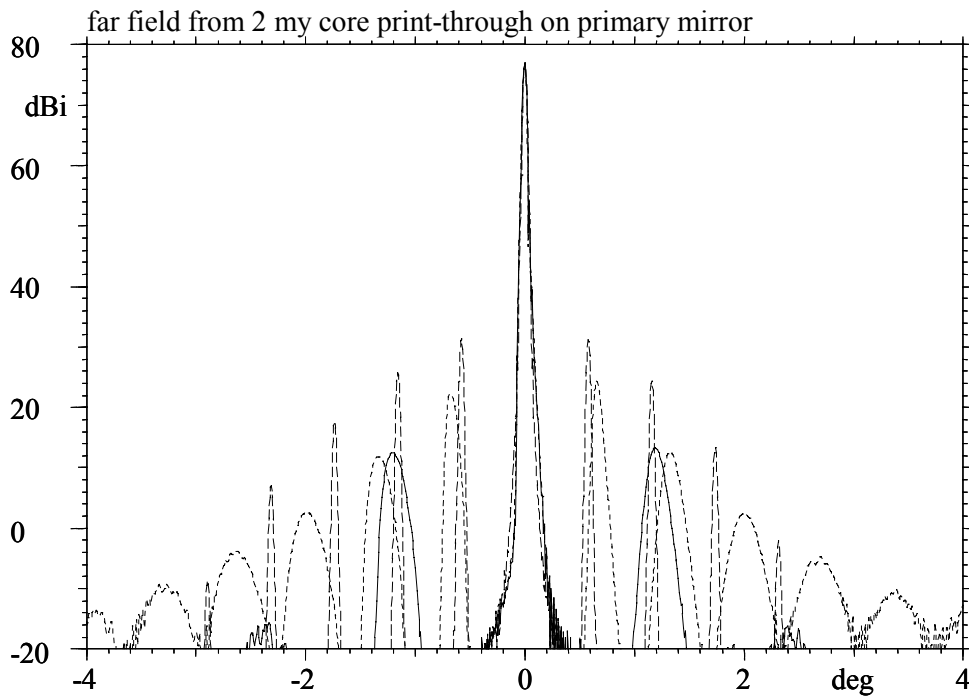
b) cuts,  $\phi = 0^\circ, 26^\circ, 90^\circ$ 

Figure 3-2 Far field from core print-through with  $10\mu$  peak on primary mirror.



a) uv pattern



b) cuts,  $\phi = 0^\circ, 26^\circ, 90^\circ$

Figure 3-3 Far field from core print-through with  $2\mu$  peak on primary mirror.

### 3.2 Distortions on secondary mirror

A  $10\ \mu$  peak core depth-through surface distortion on the secondary mirror generates the aperture field phase degradation in Figure 3-4. The  $10^\circ$  contour curve is plotted and the peak is  $19.4^\circ$ .

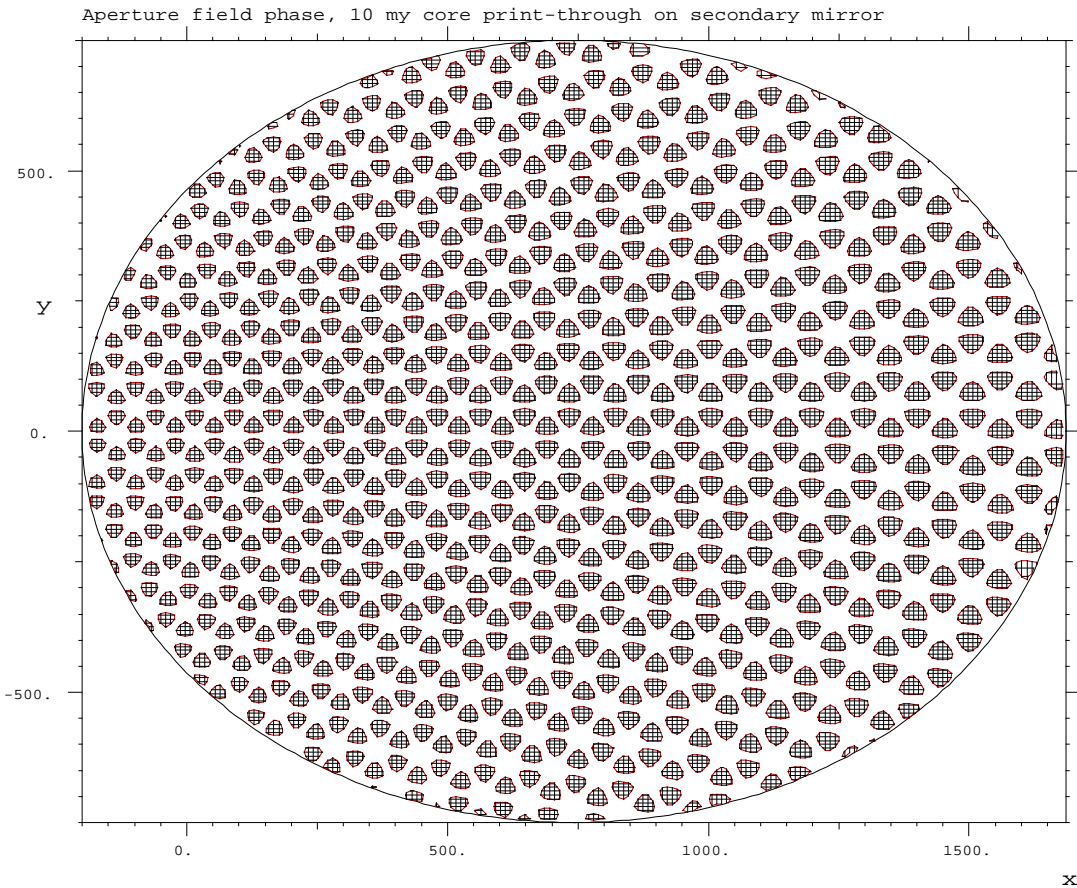
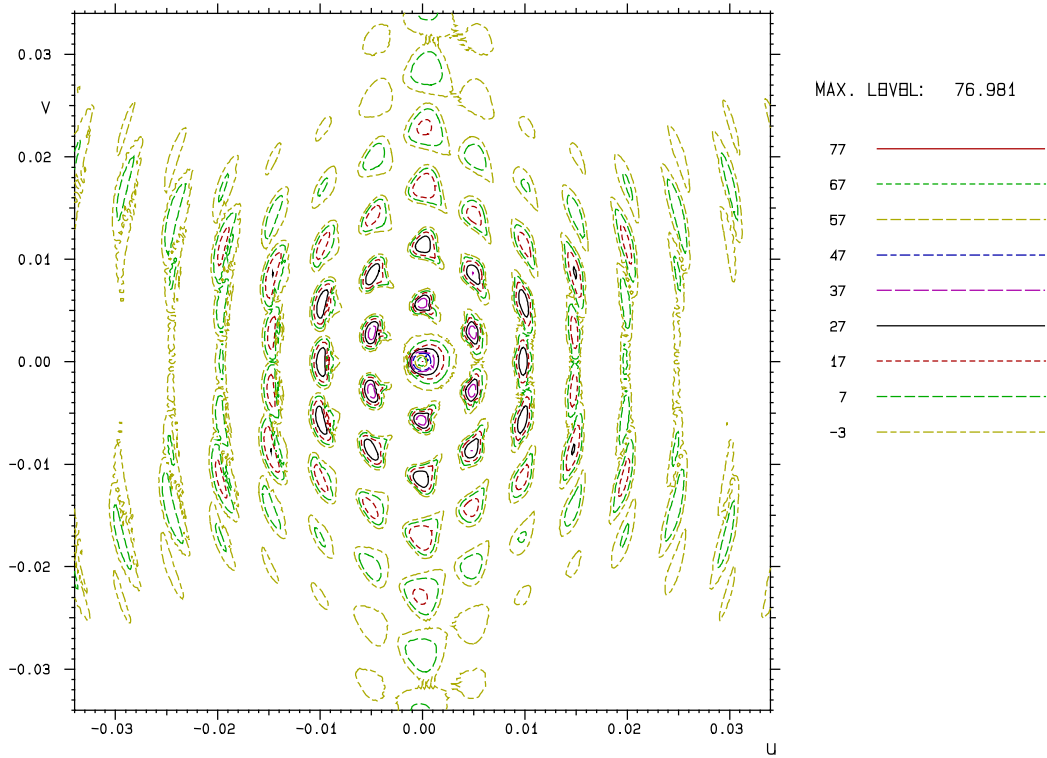


Figure 3-4 Aperture field phase error created by  $10\mu$  peak on secondary mirror.

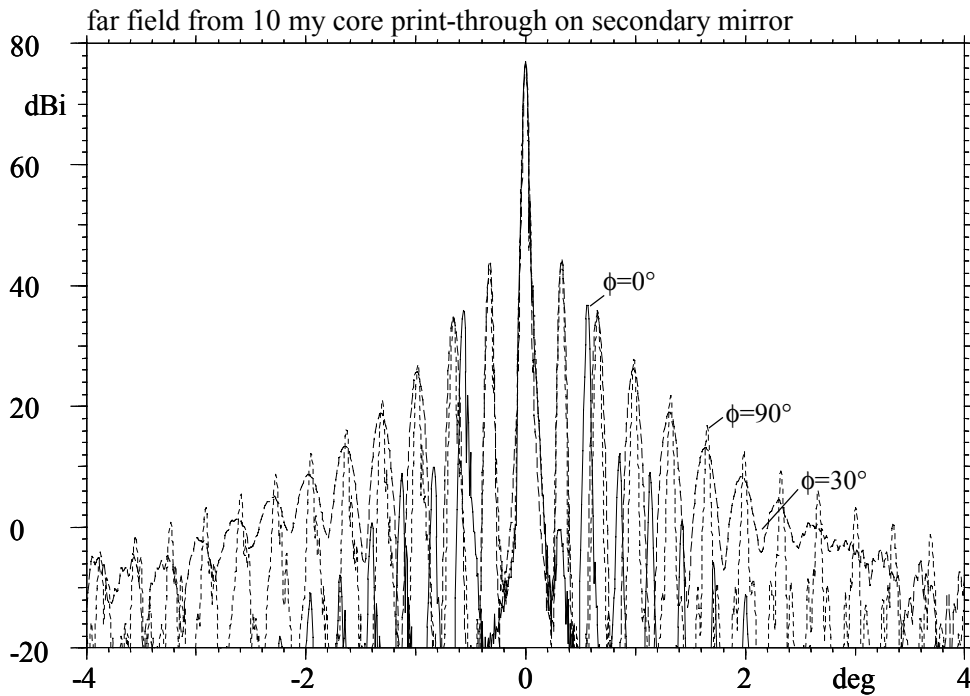
The distance between the triangles increased in the x direction due to the ray mapping from the secondary mirror. This creates the broader grating lobes in Figure 3-5a. The main beam is now reduced by 0.04 dB, and the largest grating lobe is in the  $\phi=90^\circ$ -plane at  $\theta = .33^\circ$  ( $v=.0057$ ) with a peak of 44.4 dBi, which is only 33 dB below the main peak. The most important grating lobes are shown in the three pattern cuts in Figure 3-5b in the  $\phi=0^\circ$ ,  $30^\circ$  and  $90^\circ$  planes. The S distance in the  $\phi = 0^\circ$  plane varies from 70 mm to 120 mm giving the grating lobe distance of

$\theta = .56^\circ$ . In the  $\phi = 90^\circ$  plane the S distance is 72 mm which agrees very well with the  $\theta$  value of  $.33^\circ$ .

If the core print through peak is reduced to  $2\mu$  the grating lobes are again reduced by 14 dB as shown in Figure 3-6.

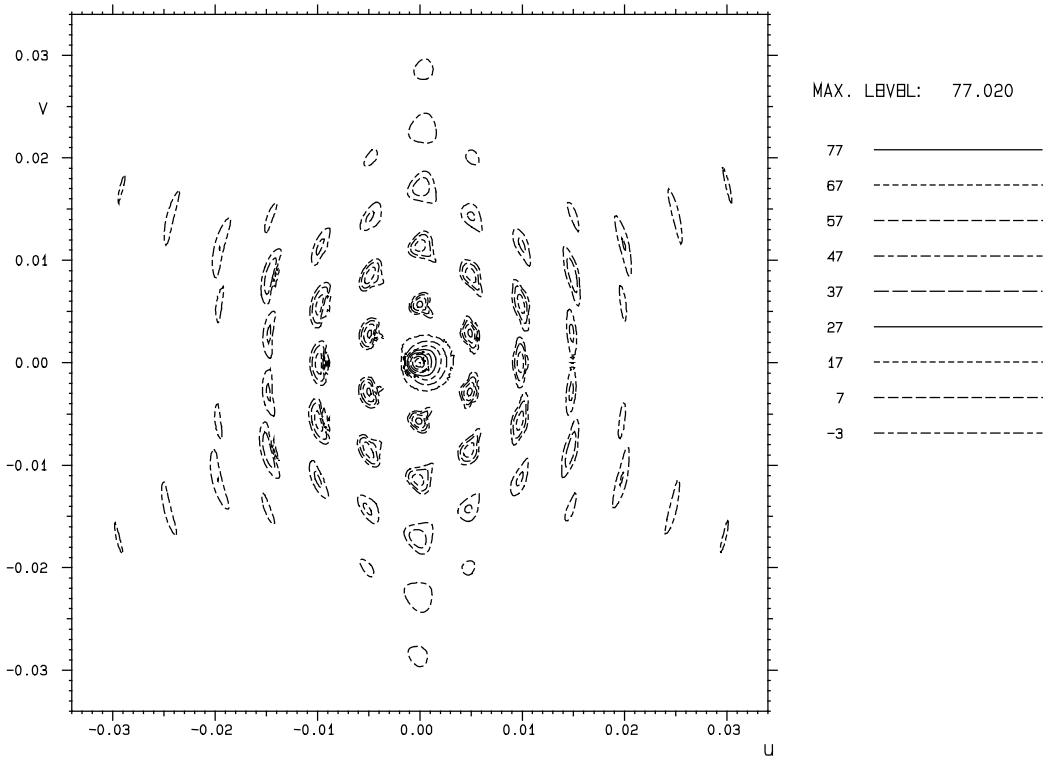


a) uv pattern

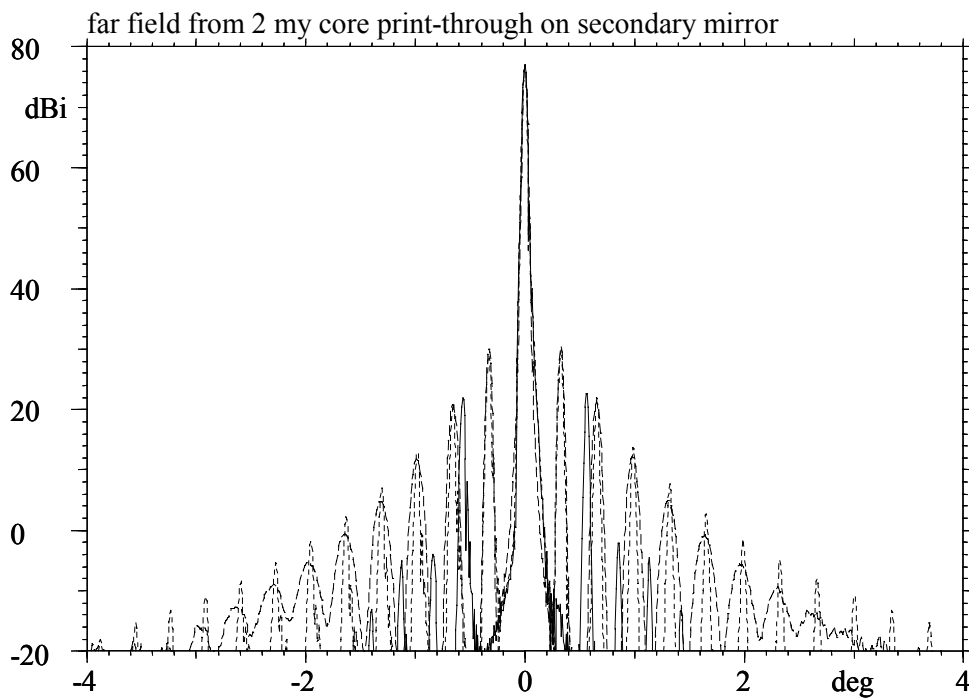


b) cuts,  $\phi = 0^\circ, 30^\circ, 90^\circ$

Figure 3-5 Far field from core print-through with 10μ peak on secondary mirror.



a) uv pattern



b) cuts,  $\phi = 0^\circ, 30^\circ, 90^\circ$

Figure 3-6 Far field from core print-through with  $2\mu$  peak on secondary mirror.

#### 4. FREQUENCY DEPENDENCE

At lower frequencies the grating lobes from the core print-through are reduced in amplitude and the scanned farther away from the main beam.

The direction of the grating lobes can be found using the equations (3.1) and (3.2), and the lobe closest to the main beam can be estimated by:

$$f_{\text{GHz}} * \sin(\theta_{\text{gr}}) \approx 8.7 \quad \text{for primary mirror distortion (4.1)}$$

and

$$f_{\text{GHz}} * \sin(\theta_{\text{gr}}) \approx 4.9 \quad \text{for secondary mirror distortion (4.2)}$$

where  $f_{\text{GHz}}$  is the frequency in GHz.

The phase degradation from the core print-through surface distortion decreases with the frequency. The value of the grating lobe amplitude below the main beam peak,  $\Delta G_{\text{gr}}$ , at  $10\mu$  core print-through therefore increases to

$$\Delta G_{\text{gr}} = 32\text{dB} + 20.*\log(857/f_{\text{GHz}}) \text{ dB} \quad (4.3)$$

Due to different aperture illuminations and different scan aberrations there may be minor variations from these simple formulas.

---

## 5. REFERENCES

ALCATEL, 26/07/1999,

"Planck Payload Module Architect Technical Assistance,  
Telescope optimisation & RF analysis". Phase 1 report.  
Doc. No. PLAS TN 009.

ESA, 01/09/1999,

Draft report. Doc. No. PT-DS-07024.

TICRA, 1999,

"RF properties of the Planck telescope, Designed by  
ALCATEL CASE No. 1". TICRA report S-801-04.